

# Solar Dynamic Concentrator Durability in Atomic Oxygen and Micrometeoroid Environments

Daniel A. Gulino\*

NASA Lewis Research Center, Cleveland, Ohio

Solar dynamic power system mirrors for use on Space Station and other spacecraft flown in low-Earth-orbit (LEO) are exposed to the harshness of the LEO environment. Both atomic oxygen and micrometeoroids/space debris can degrade the performance of such mirrors. Coatings will be required to protect oxidizable reflecting media, such as silver and aluminum, from atomic oxygen attack. Several protective coating materials have been identified as good candidates for use in this application. The durability of these coating/mirror systems after pinhole defects have been inflicted during their fabrication and deployment or through micrometeoroid/space debris impact once on-orbit is of concern. Studies of the effect of an oxygen plasma environment on protected mirror surfaces with intentionally induced pinhole defects have been conducted and are reviewed in this paper. It has been found that oxidation of the reflective layer and/or the substrate in areas adjacent to a pinhole defect, but not directly exposed by the pinhole, can occur.

## Electric-Power Generation on Space Station

**E**LECTRIC-POWER generation on the Space Station is planned to be accomplished by two means: traditional photovoltaic panels will account for about one-third of the total power generated, and solar dynamic modules will account for the other two-thirds. Solar dynamic systems generate electricity by focusing the sun's radiation, through use of either mirrors or lenses, onto the receiver of a heat engine. The current configuration<sup>1</sup> calls for a reflective system, with either aluminum or silver as the reflective medium.

Figure 1 is a schematic diagram of a solar concentrator that utilizes a mirror made up of 19 hexagonal elements that are, in turn, composed of triangular, spherically contoured facets. Figure 2 is a diagram of one of the triangular facets. The current design calls for these facets to consist of an aluminum honeycomb core with a graphite-epoxy laminate on each side. The reflective metal (most likely either aluminum or silver) is deposited onto the graphite-epoxy, followed then by the protective coating. This paper is concerned with the potential effects of the low-Earth-orbit environment on the performance of these mirrors.

## Low-Earth-Orbit Environment

The low-Earth-orbit (LEO) environment presents several hazards to the long-term survivability of large mirrors. The dominant chemical constituent between 200 and 650 km is atomic oxygen (Fig. 3),<sup>2</sup> and because both aluminum and silver are susceptible to oxidation, protection of the reflective metal from atomic oxygen attack is vital to the survivability of these mirrors.

Another potential hazard to space-borne reflectors in LEO is the particulate matter environment. Micrometeoroids, as well as other such "natural" phenomena as space debris, are a potential source of pinhole defects in the protective coating of a reflecting mirror. Other potential sources of such defects include the fabrication, handling, transport, and deployment of

the mirror facets. Once a pinhole defect has been inflicted, by whatever mechanism, a pathway is provided for direct attack of the reflective layer and/or the graphite-epoxy substrate by atomic oxygen.

## Candidate Protective Coatings

Several materials have been proposed for use as protective coatings over the reflective layer. Any material chosen for such an application must meet a number of requirements. The material must be transparent to solar radiation in the wavelength region of interest, generally 200–2500 nm. It must also be easily applied, strongly adherent, have low toxicity, and be of low cost. Finally, of course, it must be resistant to atomic oxygen. Materials proposed for such use include several metal oxides, such as aluminum oxide, silicon oxide, and indium-tin oxide. Other materials under consideration include magnesium fluoride and silicon nitride. This paper will discuss some of the experiments that have been conducted at NASA Lewis Research Center (LeRC) to determine the effectiveness of these coating materials in both the presence of and absence of intentionally introduced pinhole defects.

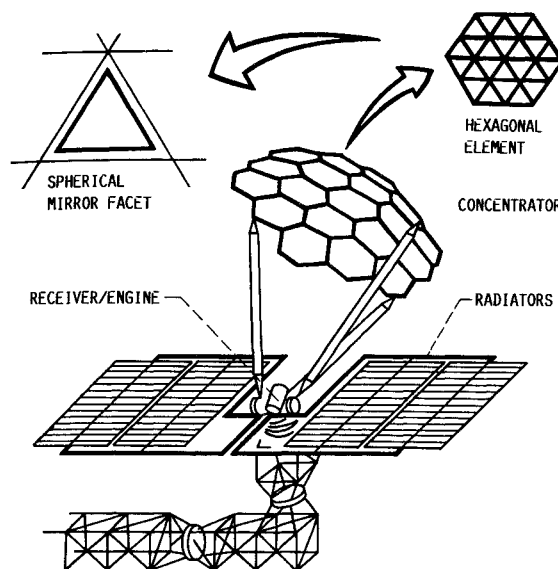


Fig. 1 Schematic of a solar dynamic module that includes a concentrator made up of hexagonal elements, each of which is comprised of spherically contoured triangular facets.

Presented as Paper. 87-0104 at the AIAA 25th Aerospace Sciences Meeting, Reno, NV, Jan. 12–15, 1987; received March 10, 1987; revision received Aug. 19, 1987. Copyright © 1987 American Institute of Aeronautics and Astronautics, Inc. No copyright is asserted in the United States under Title 17, U.S. Code. The U.S. Government has a royalty-free license to exercise all rights under the copyright claimed herein for Governmental purposes. All other rights are reserved by the copyright owner.

\*Research Scientist, Power Technology Division. Member AIAA.

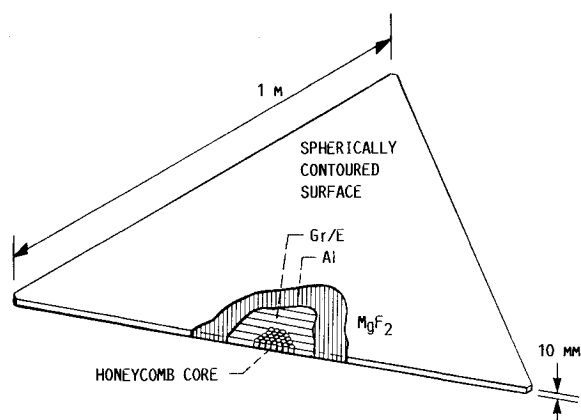


Fig. 2 One proposal for the composition of an individual facet.

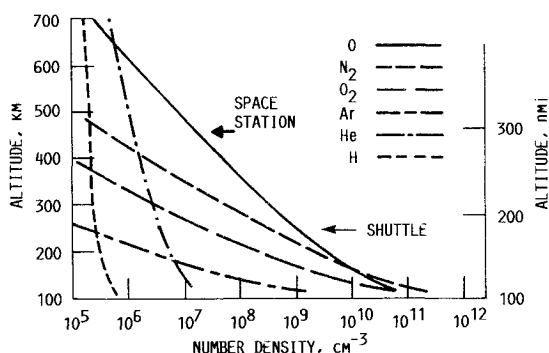


Fig. 3 Atmospheric composition as a function of altitude. The typical Shuttle orbit and proposed Space Station orbit are shown.

### Experimental Aspects

The sample mirrors studied were prepared both at LeRC and at Harris Corporation. The LeRC samples were prepared on a variety of substrate materials, including aluminum, electroformed nickel, beryllium-copper alloy, graphite-epoxy composite, and fused silica. They were fabricated by ion-beam sputtering of targets of the various protective coatings in a deposition system described elsewhere.<sup>3</sup> The Harris samples were prepared on both glass and graphite-epoxy substrates. The protective coatings were deposited by both ion-beam sputtering and electron-beam evaporation.

The atomic oxygen environment was simulated with a Structure Probe, Inc. Plasma Prep II plasma asher. This device generates a plasma by 13.56 MHz rf excitation of the carrier gas, which in all cases was ambient air. Although such information does exist for a handful of materials, direct comparisons between lifetime in the asher and lifetime in LEO are difficult; however, the asher is very useful for making gross determinations of the likelihood of survivability of a particular material in LEO. Plasma systems, in general, have found use in simulation of the LEO atomic oxygen environment.<sup>4,5</sup>

Pinhole defects were induced in protective coatings with an S.S. White Airbrasive high-speed abrasive particle system. This unit accelerated the particles, 27  $\mu$  diameter alumina in this case, to a calculated velocity of approximately 340 m/s at a flux of approximately  $6 \times 10^{12} \text{ cm}^{-2} \text{ s}^{-1}$ . This differs from the actual, LEO micrometeoroid environment in at least two important respects. First, particle velocities are considerably higher in LEO, being on the order of 10–60 km/s.<sup>6,7</sup> The effect of particle impact at velocities of this magnitude is very different. Second, micrometeoroids impacting at these velocities have been shown to become briefly fluidlike in their behavior after impact. The result is that the particle can actually line the

interior of the impact crater.<sup>7,8</sup> Thus, self-protection of the underlying material from atomic oxygen exposure as a result of the micrometeoroid itself is possible. The significance of the present experiments thus lies more in the atomic oxygen exposure response of pinhole defects (from whatever source) than in accurate micrometeoroid simulation. The effects of the hard particle impacts were characterized primarily by scanning electron microscopy.

All reflectances reported here were measured on a Perkin-Elmer Lambda-9 UV/VIS/NIR spectrophotometer equipped with a 60-mm-diam, barium sulfate-coated integrating sphere. Integrated solar reflectances were measured by obtaining the spectral reflectance over the wavelength range of 200–2500 nm and then convoluting this into the AMO solar spectrum over the same wavelength range. Both specular and total reflectances were obtained, the former of which was measured at an acceptance aperture solid angle of 0.096 steradian.

### Discussion

#### Defect-Free Samples

The effect of the asher plasma environment on the specular solar reflectance of several reflector/substrate systems is shown in Fig. 4. For comparison, the effects on an unprotected silver surface and an unprotected aluminum surface are also shown. Clearly, silver requires protection. (There is no apparent effect of substrate.) Any of the protective coatings displayed in Fig. 4 would appear to be satisfactory. Although the unprotected aluminum sample continued to have a high specular reflectance, and hence would not appear to require protection, there is concern<sup>9</sup> that the self-generated oxide layer that protects the aluminum surface would not be satisfactory. Specifically, the physical structure of aluminum oxide is such that neutral atomic oxygen could diffuse through it and continue to oxidize the aluminum surface. Thus, the oxide thickness would continuously increase, resulting in a gradual, but steady decline in specular reflectance. It may be safer and wiser to intentionally apply a coating of known thickness and properties under controlled conditions, rather than rely on the natural growth of the oxide.

Tables 1 and 2 summarize some of the experimental results that have been obtained on the effect of the asher plasma on various protective coating/reflective layer/substrate combinations. For comparison purposes, a quantity defined as the fractional loss of reflectance per unit asher exposure time was developed as a way of comparing the relative degree of protection afforded the reflecting layer by the various protective coatings. Although this quantity is based only on the start and end values of reflectance, it does give qualitatively useful information. In general, the spectral reflectance losses contributing to the tabulated losses in solar reflectance occurred over most or all of the 200–2500 nm wavelength range.

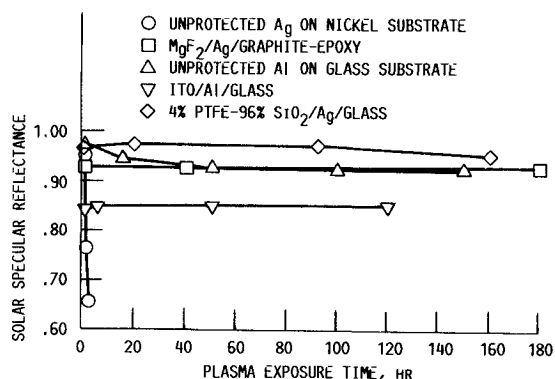


Fig. 4 Integrated solar specular reflectance as a function of plasma exposure time for several reflector systems. (Description of samples is coating material/reflecting material/substrate.)

**Table 1** Change in integrated solar reflectance of silver mirror samples with various protective coatings deposited on various substrate materials

Substrate	Protective coating	Asher exposure time, h	Solar specular reflectance		Fractional loss of solar specular reflectance per 1000 h
			Start	Finish	
Nickel	—	2.1	0.952	0.654	142
Nickel	<sup>a</sup> Al <sub>2</sub> O <sub>3</sub>	75	0.911	0.911	0
Nickel	<sup>a</sup> Si <sub>3</sub> N <sub>4</sub>	400	0.916	0.881	0.088
Glass	<sup>a</sup> SiO <sub>2</sub>	634	0.972	0.937	0.055
Glass	<sup>a</sup> SiO <sub>2</sub> / <sup>b</sup> MgF <sub>2</sub>	634	0.970	0.927	0.068
Glass	<sup>a</sup> ITO	225	0.899	0.908	—
Glass	<sup>a</sup> ITO/ <sup>b</sup> MgF <sub>2</sub>	225	0.925	0.902	0.102
Glass	PTFE — <sup>a</sup> SiO <sub>2</sub>	159	0.971	0.951	0.126
Gr/Epoxy	<sup>a</sup> SiO <sub>2</sub>	180	0.945	0.910	0.194
Gr/Epoxy	<sup>b</sup> MgF <sub>2</sub>	180	0.930	0.925	0.028
Be/Cu alloy	<sup>a</sup> SiO <sub>2</sub>	62	0.914	0.859	0.887

<sup>a</sup>Coatings deposited by ion-beam sputtering.<sup>b</sup>Coatings deposited by vacuum evaporation.**Table 2** Change in integrated solar reflectance of aluminum mirror samples with various protective coatings deposited on various substrate materials

Substrate	Protective coating	Asher exposure time, h	Solar specular reflectance		Fractional loss of solar specular reflectance per 1000 h
			Start	Finish	
Glass	—	150	0.976	0.931	0.300
Glass	<sup>b</sup> MgF <sub>2</sub>	150	0.927	0.927	0
Glass	<sup>a</sup> SiO <sub>2</sub>	634	0.891	0.879	0.019
Glass	SiO <sub>2</sub> / <sup>b</sup> MgF <sub>2</sub>	634	0.882	0.834	0.076
Glass	<sup>a</sup> ITO	225	0.850	0.844	0.027
Glass	<sup>a</sup> ITO/ <sup>b</sup> MgF <sub>2</sub>	225	0.847	0.815	0.142
Gr/Epoxy	<sup>b</sup> MgF <sub>2</sub>	180	0.925	0.910	0.083

<sup>a</sup>Coatings deposited by ion-beam sputtering.<sup>b</sup>Coatings deposited by vacuum evaporation.**Samples with Pinhole Defects**

Figures 5–13 present results showing the effect of pinhole defects on the asher plasma environment durability of both silver and aluminum reflecting surfaces with protective coatings on both graphite-epoxy composite and fused quartz substrates. The protective coatings for most of the samples consisted of 700 Å of Al<sub>2</sub>O<sub>3</sub> followed by 2200 Å of SiO<sub>2</sub>. The generally observed effect is that oxidation of the reflective layer and/or the substrate occurs in undamaged areas surrounding a defect site.

In the case of mirror samples constructed on oxidizable (graphite-epoxy) substrates, oxidation of both the reflecting layer and the substrate surrounding the defect occurs. Figure 5 shows a silver mirror surface with intentionally induced pinhole defects. A number of the defect sites are visible. Figure 6 shows a similar surface after 90 h of exposure in the plasma asher. Several of the defect sites are now surrounded by a discolored (in this case, darkened) border. These discolored areas are the result of oxidation of the silver and/or the graphite-epoxy substrate in the area surrounding the defect site. Figure 7 shows a similar effect, but through an elongated defect.

Figure 8 shows an eroded surface after approximately 240 h of plasma asher exposure. Oxidative undercutting occurred to a large extent in this sample. The discolorations now cover a substantial portion of the total sample surface area. Figure 9 shows the lower right portion of Fig. 8, but at a higher magnification and a higher (60 deg) angle of tilt. It can be seen that wherever there are discolorations, the surface of the coating had become distorted (caved in). This is most likely caused by

the release of the intrinsic compressive stress in the film due to loss of the substrate support.

Sample mirrors constructed on fused silica substrates showed different but related oxidative behavior. Figure 10 depicts a silver reflector sample on a fused silica substrate after about 50 h of plasma asher exposure. Here can be seen a light-colored, puffed material protruding through almost every defect site. This material is oxidized silver expanding in the only direction available, which is through the defect opening. Unlike graphite-epoxy, fused silica does not oxidize in the asher environment. Hence, no space is created beneath the coating by oxidation of the substrate. Figure 11 shows the same surface as seen in Fig. 10, but at a 60 deg angle of tilt. Here, the extent of growth of the oxide through the opening is more easily appreciated.

Figure 12 shows a surface similar to that of Fig. 10, but after approximately 240 h of exposure. Silver oxide protruding through the defect is again clearly seen. In addition, oxidative undercutting (perhaps more descriptively referred to as "transverse oxidation") of the silver layer beneath the protective coating is seen, as in Fig. 6, as a discolored (in this case, lighter) border surrounding the defect. The extent of undercutting is not, however, as great as on the graphite-epoxy substrate samples.

A brief discussion of the difference in "color" of oxidative undercutting in one case and transverse oxidation in the other is in order. In the former, we are looking at what is primarily oxidation of the graphite-epoxy substrate (actually, we are probably looking at graphite-epoxy itself, since the oxidation products are most likely volatiles that would outgas upon for-

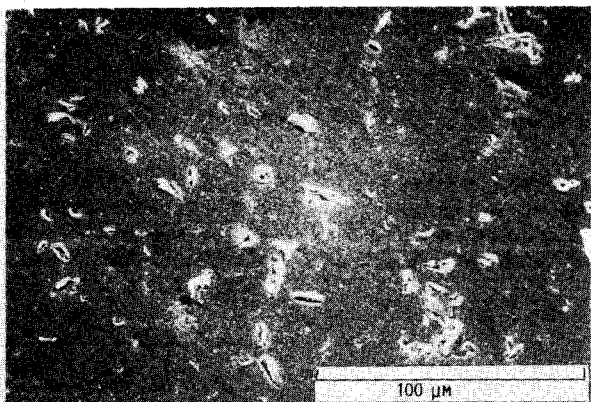


Fig. 5 Defects due to particle erosion. The reflective system is  $\text{SiO}_2/\text{Al}_2\text{O}_3/\text{Ag}/\text{graphite-epoxy}$ .

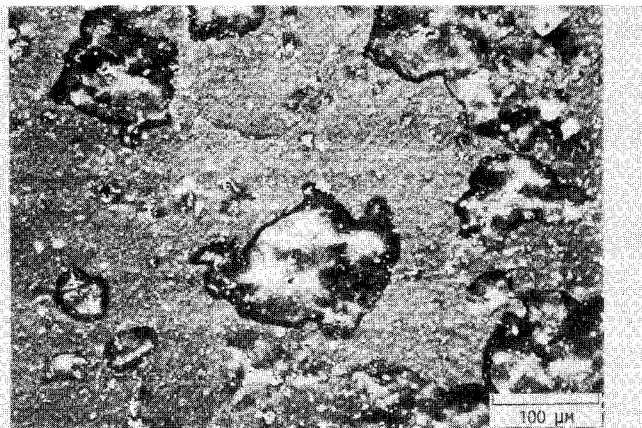


Fig. 8 Particle-eroded surface of a sample identical to that of Fig. 5 after 240 h of plasma asher exposure. Oxidative undercutting has occurred to a large extent.

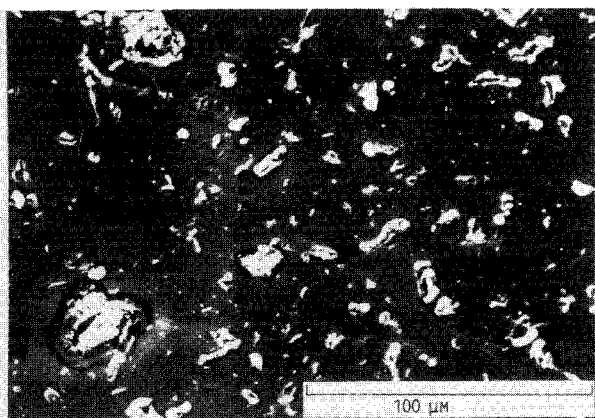


Fig. 6 Particle-eroded surface of a sample identical to that of Fig. 5 after 90 h of plasma asher exposure. Several defect sites are surrounded by discolored borders, which indicate oxidation beneath the protective coating.

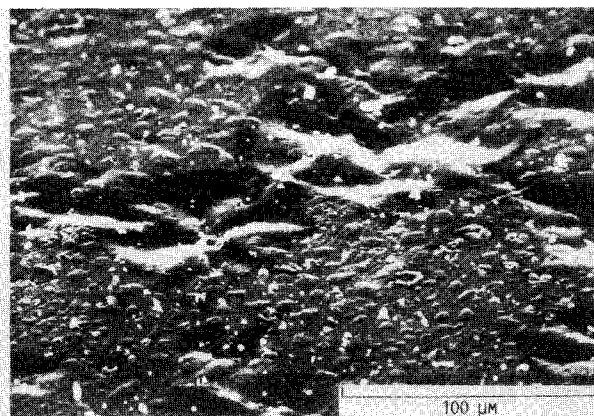


Fig. 9 Lower right portion of Fig. 8 taken at a high tilt angle (60 deg). Wherever oxidative undercutting occurred, the surface had become distorted.



Fig. 7 Surface of a sample identical to that of Fig. 5 after 90 h of plasma asher exposure. Oxidative undercutting around the elongated defect is clearly visible.

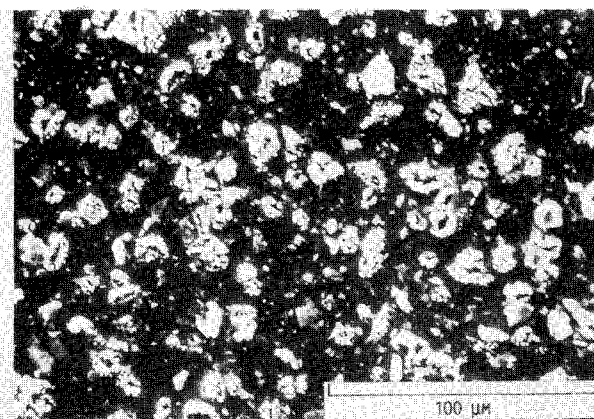


Fig. 10 Eroded surface on a fused silica substrate after 50 h of plasma asher exposure. The protective coating is  $\text{SiO}_2/\text{Al}_2\text{O}_3$ . Oxidized silver protruding through the defect sites can be seen.

mation), whereas in the latter the oxidation is strictly that of silver. It is not unreasonable to assume that the oxidation products of these two materials will have differing electrical conductivities. Since electron microscopy relies on differing electrical conductivities to form an image, it is reasonable to conclude that these oxidation products will appear differently in an electron microscope image.

Clearly, a protective coating cannot continue to protect indefinitely after pinhole defects have been introduced. Oxidative damage goes beyond what would normally be expected to oc-

cur as a result of the presence of the pinholes themselves. As pointed out earlier, there is a difference between how the pinhole defects were produced in these samples (low-velocity impact by particles of constant size and composition) and the actual result of a micrometeoroid impact in LEO (high-velocity particles of many different sizes<sup>10</sup> and of varying composition). Also, as stated earlier, self-protection is possible.

Results from the analysis of the Solar Maximum Mission spacecraft by Laurance and Brownlee<sup>11</sup> provide an interesting comparison to the data presented here. This satellite was recov-

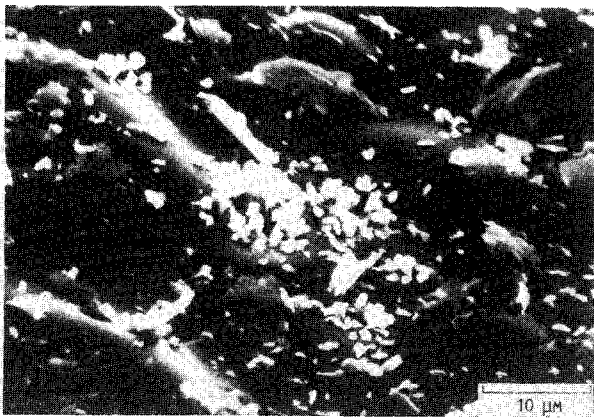


Fig. 11 Same surface as that of Fig. 10, but at a higher magnification and at a higher angle of tilt (60 deg). The extent of oxidation of the silver is more easily seen.

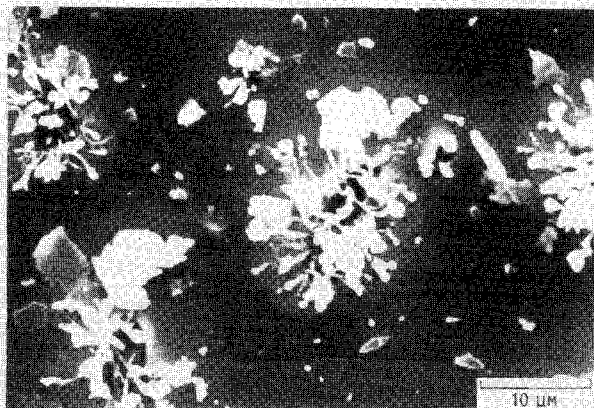


Fig. 12 Eroded surface of sample identical to that of Fig. 10 after 240 h of plasma exposure. Silver oxide protruding through the defect sites is clearly seen. In addition, transverse oxidation of the silver layer beneath the protective coating is seen as a lighter border surrounding the defect sites.

ered on April 10, 1984 by the crew of Space Shuttle flight 41-C. The satellite had been exposed to the space environment at altitudes ranging from 500–570 km for a period of 4.15 years. Examination of the satellite's aluminum thermal control louvers revealed craters ranging in size from 0.1–250  $\mu$ . Analysis of the residue found in the craters indicated that the particles arose from both the natural environment and the remains of man-made spacecraft. The cumulative flux of particles equal in mass to or heavier than that used in the present work is quite low, being on the order of  $10^{-6} \text{ m}^{-2} \text{ s}^{-1}$ . The flux increases as particle size diminishes, but it is difficult to predict at what point the mass of the particles would become too small to penetrate the protective coating. Nonetheless, these data indicate that solar concentrator mirrors should be relatively safe from damage from particles as large as those used here.

In light of the foregoing, the usefulness of the results discussed here is primarily in the effect of pinhole defects on the continued atomic oxygen durability of protected mirror surfaces. Other possible sources of pinholes exist, and these include the fabrication, transport, and deployment of large mirrors. Figure 13 illustrates this point. It shows an aluminum reflector on a graphite-epoxy substrate with a  $\text{MgF}_2$  protective coating after about 270 h of exposure. The defect shown was not intentionally induced, but was present simply as a result of the fabrication or handling of the sample. It is clear that oxidation of the substrate surrounding the defect has occurred.

Figure 14 is a schematic diagram showing both the oxidative undercutting and the related, transverse oxidation processes

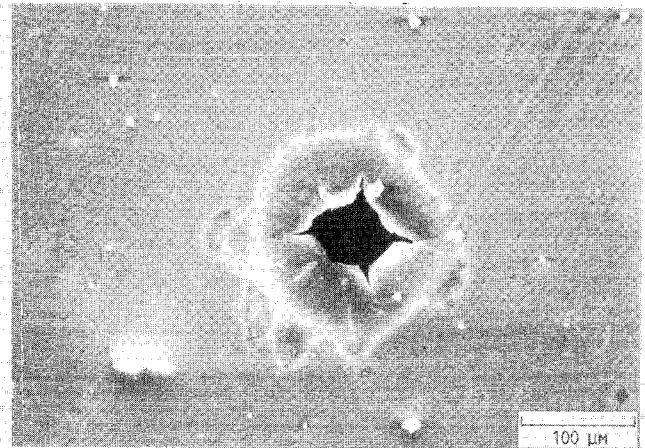


Fig. 13 Aluminum reflector after 270 h of plasma asher exposure. The protective coating was  $\text{MgF}_2$  and the substrate was graphite-epoxy. The defect shown was not intentionally induced, but was created during the fabrication or handling of the sample. Oxidative undercutting has occurred.

just discussed. Figure 14a depicts oxidative undercutting. Here, the atomic oxygen passes through the defect site and erodes both the reflective layer and the substrate around the opening. This process apparently leaves sufficient space for the growing, expanding oxide, as none was seen protruding through the defect sites in the graphite-epoxy substrate samples. Figure 14b depicts transverse oxidation. Here, the atomic oxygen passes through the defect site and oxidizes only the silver reflective layer. Since in this case the substrate is not oxidizable, the expanding silver oxide has no place to go but out through the defect. It would also be expected that the rate of transverse oxidation would be slower than that of oxidative undercutting, since the protruding oxide would tend to hinder the diffusion of the atomic oxygen to the oxidation front between the oxidized and elemental silver. This slower rate was observed in the relative sizes of the discolored borders (discussed here) between the graphite-epoxy (larger border) and fused silica (smaller border) substrate samples.

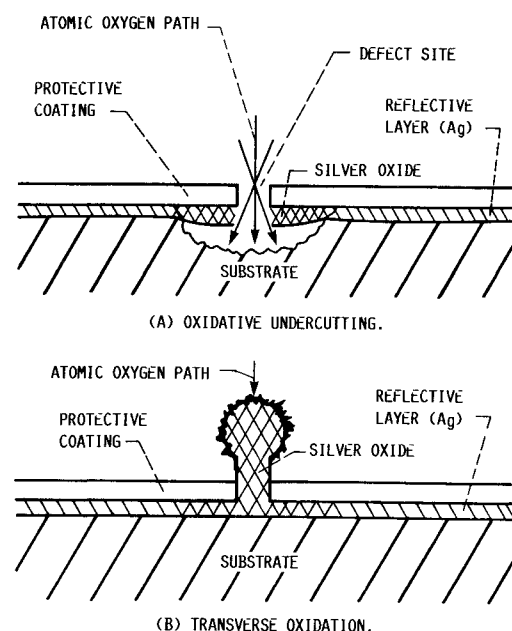


Fig. 14 Schematic representation of oxidative undercutting of both the reflective layer and substrate when the substrate itself is susceptible to oxidation a), and of transverse oxidation of the reflective layer alone when the substrate is resistant to oxidation b).

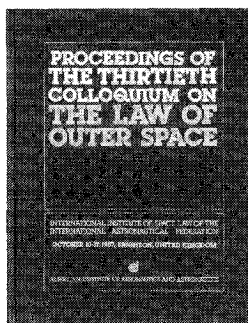


### Conclusions

In this paper, an attempt has been made to indicate the effects of a LEO environment on the durability of space-borne reflecting mirrors. Atomic oxygen presents a hazard to silver and aluminum solar dynamic power system reflectors. Therefore, protective coatings are necessary to prevent atomic oxygen degradation of these metals. Several suitable candidates have been identified and discussed here. Pinhole defects, resulting from a variety of possible causes, are pathways for direct atomic oxygen attack of both the reflective metal and the substrate. It has been found that atomic oxygen degradation is not confined to that portion of the reflector surface directly exposed as a result of the presence of the pinhole. Oxidation of the reflecting layer and/or the substrate can occur. The effect of this process on the long-term, on-orbit performance of large mirror needs to be determined.

### References

- <sup>1</sup>"Solar Concentrator Advanced Development Program, Task 1 Final Report," Harris Corp., Melbourne, FL, June 1986; also, NASA CR-179489, 1986.
- <sup>2</sup>Peplinski, D. R., Arnold, G. S., and Borson, E. M., "Introduction to: Simulation of Upper Atmosphere Oxygen—Satellite Exposed to Atomic Oxygen in Low Earth Orbit," 13th Space Simulation Conf., NASA CP-2340, 1984, pp. 133-145.
- <sup>3</sup>Gulino, D. A., "Ion Beam Sputter Deposited Zinc Telluride Films," *Journal of Vacuum Science and Technology*, Vol. A4, May/June 1986, pp. 509-513.
- <sup>4</sup>McCargo, M., Dammann, R. E., Robinson, J. C., and Milligan, R. J., "Effects of Combined Ultraviolet and Oxygen Plasma Environment on Spacecraft Thermal Control Materials," *Proceedings of the International Symposium on Environmental and Thermal Systems for Space Vehicles*, European Space Agency SP-200, 1983, pp. 447-451.
- <sup>5</sup>Fromhold, A. T., Jr., Noh, S., Beshears, R., Whitaker, A. F., and Little, S. A., "Theoretical Approach to Oxygen Atom Degradation of Silver," *Proceedings of the NASA Workshop on Atomic Oxygen Effects*, JPL Publication 87-14, 1987, p. 163.
- <sup>6</sup>Mirtich, M. J. and Mark, H., "Alteration of Surface Optical Properties by High Speed Micron-Size Particles," *Symposium on Thermal Radiation of Solids*, NASA SP-55, edited by S. Katzoff, 1964, pp. 473-481.
- <sup>7</sup>Merril, R. B., "The Effects of Micrometeoroids on the Emittance of Solids," *Symposium on Thermal Radiation of Solids*, NASA SP-55, edited by S. Katzoff, 1964, pp. 453-472.
- <sup>8</sup>Mirtich, M. J. and Mark, H., "The Effect of Hypervelocity Projectile Material on the Ultimate Reflectance of Bombarded Polished Metals," NASA TM X-52981, 1971.
- <sup>9</sup>"Conceptual Design Definition and Analysis of a Reflective Surface and Substrate, Vol. II—Study Results," Acurex Corp., Mountain View, CA, FR-85-168/EE, Dec. 1985.
- <sup>10</sup>Smith, R. E. and West, G. S., "Space and Planetary Environment Criteria Guidelines for Use in Space Vehicle Development," Vol. 1, 1982 Revision, NASA TM-82478, 1983.
- <sup>11</sup>Laurance, M. R. and Brownlee, D. E., "The Flux of Meteoroids and Orbital Space Debris Striking Satellites in Low Earth Orbit," *Nature*, Vol. 323, Sept. 1986, pp. 136-138.



## PROCEEDINGS OF THE THIRTIETH COLLOQUIUM ON THE LAW OF OUTER SPACE

International Institute of Space Law of the International  
Astronautical Federation, October 10-17, 1987, Brighton, England  
**Published by the American Institute of Aeronautics and Astronautics**

1988, 426 pp. Hardback  
ISBN 0-930403-40-1  
Members \$29.50 Nonmembers \$59.50

**B**ringing you the latest developments in the legal aspects of astronautics, space travel and exploration! This new edition includes papers in the areas of:

- Legal Aspects of Maintaining Outer Space for Peaceful Purposes
- Legal Aspects of Outer Space Environmental Problems
- Legal Aspects of Commercialization of Space Activities
- The United Nations and Legal Principles of Remote Sensing

You'll receive over 60 papers presented by internationally recognized leaders in space law and related fields. Like all the IISL Space Law Colloquiums, it is a perfect reference tool for all aspects of scientific and technical information related to the development of astronautics for peaceful purposes.

**To Order:** Write AIAA Order Department, 370 L'Enfant Promenade, S.W., Washington, DC 20024. All orders under \$50.00 must be prepaid. Please include \$4.50 for postage and handling. Standing orders available.